Available online at www.sciencedirect.com

ScienceDirect

Nuclear Physics A 1037 (2023) 122700

NUCLEAR PHYSICS A

www.elsevier.com/locate/nuclphysa

# Description of temperature effects on proton radioactivity

R. Gharaei [a,*], M. Jalali Shakib [a], K.P. Santhosh [b,c]

[a] *Department of Physics, Sciences Faculty, Hakim Sabzevari University, P. O. Box 397, Sabzevar, Khorasan Razavi, Iran*
[b] *School of Pure and Applied Physics, Kannur University, Swami Anandatheertha Campus, Payyanur 670327, Kerala, India*
[c] *Department of Physics, University of Calicut, Kerala 673635, India*

Received 7 November 2022; received in revised form 13 May 2023; accepted 1 June 2023

**Abstract**

Role of thermal effects of hot parent nuclei in the characteristics of proton emission process has been studied for the first time by analyzing the surface energy coefficient $\gamma$ entering in the calculation of proximity potential for 15 experimentally detected proton emitters ($67 \leq Z \leq 83$) in the isomeric states. In the present work, the proton-nucleus interaction potentials are obtained by using one of the latest versions of proximity potential formalism proposed by Zhang et al. in 2013. In addition, the quantum mechanical tunneling probability and consequently the proton radioactivity half-lives are calculated within the framework of the semiclassical WKB method. We present a new temperature-dependent (TD) form of the coefficient $\gamma$ based on thermal properties of hot proton emitters in the framework of the finite-temperature generalized liquid-drop model. By integrating temperature dependence into the surface energy coefficient of proximity potential Zhang 2013, a reasonable description of the experimental half-lives of proton radioactivity is achieved. We extend the modified form of the Zhang 2013 model to predict the proton radioactivity half-lives of 6 proton emitters in the isomeric states, whose proton radioactivity is energetically allowed or observed, but has not been quantified yet. The obtained results reveal that the predictions by our model are in good agreement with the other theoretical methods, namely UDLP proposed by Qi et al. (2012) [19] and NGNL proposed by Chen et al. (2019) [49]. In this work, we also attempt to introduce an empirical formula for estimating the half-lives of one-proton emission process from the excited states by taking into account both the thermal effects of all the available 15 hot proton emitters and the contribution of centrifugal potential. Our results indicate that the calculated proton radioactivity half-lives by the current formula are in good agreement with experimental data. This means that the correlation between the half-lives of proton

* Corresponding author.
*E-mail addresses:* r.gharaei@hsu.ac.ir (R. Gharaei), drkpsanthosh@gmail.com (K.P. Santhosh).

https://doi.org/10.1016/j.nuclphysa.2023.122700

decay processes and the nuclear temperature $T$ of proton emitters can be suitable to deal with the proton radioactivity one-proton transition from isomeric states.


*Keywords:* Proton decay; Thermal effects; Half-life

## 1. Introduction

In recent years, one of the principal objectives that has been attracted a lot of attention in the case of nuclei located very far from the beta stability line is the observation of many new radioactive decay modes. This reality brought impressive progress in studying properties of such exotic nuclides [1–3]. The half-life, possible radioactive decay modes, and relative probabilities are the most fundamental properties of unstable nuclides that are usually established first. The study of proton radioactivity as an important decay mode has been become a topic of interest in contemporary nuclear physics. In 1970, the experimental evidence of proton radioactivity was firstly reported by detecting the emission of a proton from the isomeric state of $^{53}$Co to the ground state of $^{52}$Fe [4,5]. Since then, the proton radioactivity has been observed for different nuclei in the range of mass number $A = 108$ to 185 with the charge numbers spanning between 53 to 83. What needs to be emphasized is that proton radioactivity is a typical decay mode of odd-$Z$ nuclei beyond the proton drip line. In being an analogous phenomenon to the emission of alpha decay, the process of proton radioactivity can be dictated by a positive $Q$-value for its spontaneous emission. Moreover, the concept of proton emission can extract some important information on the nuclear structures and properties of proton-rich nuclei, such as the shell structure [6] and the internuclear interaction potential [7–11]. It should be noted that some proton emitters are spherical and some are deformed (either prolate or oblate). So far, several theoretical approaches have been put forward to analyze the proton decay process of spherical and deformed proton emitters which can certainly be utilized to obtain information on nuclear structure. In 2016 [12], as an example, the half-lives of various proton emitters have been systematically studied within the framework of the deformed density-dependent model. In that study, the authors proposed an analytical expression to obtain the proton radioactivity half-lives based on the one-dimensional Wentzel-Kramers-Brillouin (WKB) semiclassical approximation plus the deformation effect. It is found that the theoretical calculations are in satisfactory agreement with the experimental values and also with other theoretical studies. As another example, in 2018 [13], the half-lives of proton emissions have been predicted for even and odd $Z$ nuclei with $Z = 100 - 136$ using the Coulomb and proximity potential model for deformed nuclei (CPPMDN). The authors obtained a new relation for proton decay half-lives from the observed variation of Geiger-Nuttall law with respect to the $Z$ value of the parent nucleus. The obtained results show that the half-lives evaluated using CPPMDN are closer to those obtained using the new relation than the Coulomb and proximity potential model (CPPM), in which both the parent and daughter nuclei are treated as spherical. From a physical standpoint, the theoretical interpretation of the process of proton emission is similar to alpha decay [14], in that both charged particles penetrate through a Coulomb barrier as a typical result of a quantum tunneling phenomenon. It is well known that this potential barrier is composed of the nuclear, Coulomb and centrifugal potentials. In this situation, one can find that the proton radioactivity can be dealt with the WKB approximation. Within the framework of this approximation, the existence of a suitable analytical form for estimating the

emitted proton-daughter nucleus nuclear potential plays a key role for calculating the barrier penetrability and thus the half-lives of proton emitters as accurately as possible. Up to now, various theoretical approaches have been developed to study this issue such as the generalized liquid-drop model [7,15], the Woods-Saxon-type potential [16,17], the single-folding model [18], the universal decay law of proton radioactivity [19], the modified two-potential approach [20] and the phenomenological unified fission model [21,22]. The proximity formalism [23] is one of the useful tools to study the properties of the natural radioactivity of unstable nuclei [10,24–29]. Generally, the proximity potential is based on the fact that when the two nuclei approach each other within a distance of few fermi, 2-3 fm, then an additional force acts due to the surfaces proximity. It is clear from the existing literature, this formalism allows us to investigate the role of various physical effects in the interaction potential and ultimately in the $\alpha$-particle and heavier-cluster decays of radioactive nuclei [24,30–33]. Accordingly, during the past few years, several theoretical approaches have been proposed to analyze the influence of surface energy coefficients as well as thermal energy variation on the geometric configuration of the dinuclear system and thus on the calculations of the emitted $\alpha$-core interaction potential. For example, Daei et al. [30] examined the temperature-dependent alpha decay half-lives of 344 isotopes of nuclei with the atomic number between $Z = 80$ and $Z = 102$ using the proximity model denoted as Dutt 2011 with a modified temperature dependent surface energy coefficient as follows,

$$\gamma(T) = \gamma(T=0)\left[1 - 0.07T\right]^2 \ \mathrm{MeV.fm^{-2}}. \tag{1}$$

The obtained results reveal that a considerable improvement in the $\alpha$-decay half-lives can be obtained by incorporating the temperature dependence of the surface energy coefficient, using Eq. (1), in the proximity formalism.

Up to now, about 44 proton emitters have been experimentally identified over a wide mass region of $108 \leq A \leq 185$ (with the charge number between $Z = 53 - 83$). Of the known proton emitters, 15 parent nuclei emit protons from their low-lying excited or isomeric state transitions, while 29 other cases are observed as ground states. On the other hand, the excitation energy of the parent nuclei can be responsible for the rapid increase in nuclear temperature [31,34] and thus the nuclei are known as hot nuclei. In this situation, it will be interesting to perfom a systematic study on the proton radioactivity half-lives of 1p-proton transition from isomeric states by taking into account the thermal effects of hot parent nuclei. Therefore the main intentions of the present work are summarized as follows. (i) We intend to establish a procedure for analyzing the temperature effects on the natural radioactivity of proton-rich nuclei via a new TD form of the surface energy coefficient $\gamma(T)$ in one of the latest versions of the proximity potential proposed by Zhang and co-workers in 2013 [27]. It must be noted that the "Zhang 2013" version of the proximity potential has been introduced by analyzing different alpha-decay process of natural alpha emitters. Using the present theoretical procedure, we study for the first time the temperature effects of the parent nuclei on the effective nuclear potential between the emitted proton and the daughter nucleus, transmission probability through the potential barrier and proton decay half-lives. In the previous studies, the authors analyzed the effects of nuclear deformation on the calculation of proton emission half-lives using CPPMDN [35,36]. In this approach, the interaction potential between a deformed and spherical nucleus can be constructed by taking into account the deformed two-term proximity potential proposed by Baltz and Bayman [37]. Note that the dependence on surface energy coefficient $\gamma$ has not taken into account in this potential. So it seems that the simultaneous study of the thermal effects of the proton-unstable nuclei through the coefficient $\gamma$ and their nuclear deformation effects is not still possible. (ii) By in-

vestigating the thermal variation of the logarithmic half-lives $\log_{10}T_{1/2}$ (s) of the experimental data, we try to first propose an empirical formula for the half-life estimates of 15 experimentally observed proton emitters in the isomeric state. It is the relation of the known experimental data of proton radioactivity half-life, the temperature values $T$ of hot parent nuclei, the atomic number of the daughter nuclei $Z_d$ and the orbital angular momentum $\ell$ carried away by the emitted proton particles.

This paper is organized as follows. The details of the calculations of the total proton-core interaction potential and proton radioactivity half-life are presented in Sec. 2. In Sec. 3, we discuss briefly the validity of the proximity potential Zhang 2013 to study the proton decay process. In the next step, we present a new method for analyzing the thermal effects of hot proton emitters on the one-proton transition from isomeric states. In this section, the theoretical procedure used to introduce an empirical formula for the half-lives of hot proton emitters are presented. We also test the quality of the presently obtained formula for reproducing the known experimental values. A comparison with the other model predictions is performed in Sec. 3. Finally, the summary and conclusions of the present study are presented in Sec. 4.

## 2. Theoretical framework

It is well known that the total interaction potential between the daughter nucleus and the proton particle can be defined as follows

$$V_{\rm tot}(r) = V_N(r) + V_C(r) + V_\ell(r), \tag{2}$$

where $r$ is the distance from the center to the center of the daughter nucleus and the emitted proton. To calculate the emitted proton-daughter nucleus Coulomb potential, we use the following familiar form,

$$V_C(r) = Z_p Z_d e^2 \begin{cases} \frac{1}{r}, & \text{for } r > R, \\ \frac{1}{2R}\left[3 - \left(\frac{r}{R}\right)^2\right], & \text{for } r < R, \end{cases} \tag{3}$$

where $Z_p$ and $Z_d$ is atomic number of emitted proton and daughter nucleus, respectively. In addition, $R = R_p + R_d$ where $R_p$ and $R_d$ denote the radii of emitted proton and daughter nucleus, respectively. Since $\ell(\ell+1) \rightarrow (\ell+\frac{1}{2})^2$ is a necessary correction for one-dimensional problems [38], we adopt the Langer modified form to obtain the $\ell$-dependent centrifugal potential $V_\ell(r)$ as follows,

$$V_\ell(r) = \frac{\hbar^2(\ell+\frac{1}{2})^2}{2\mu r^2}, \tag{4}$$

where $\mu$ represents the reduced mass of the proton-daughter nucleus system. Here, $\ell$ is the angular momentum carried away by the emitted proton and can be obtained by the conservation laws of spin and parity. In the present study, we select one of the latest and applicable versions of the proximity potential denoted as Zhang 2013 [27] to calculate the proton-daughter nucleus nuclear potential $V_N(r)$. According to this model, the nuclear component of the interaction potential can be written as,

$$V_N(r) = 4\pi\gamma b \frac{R_p R_d}{R_p + R_d}\left[\frac{p_1}{1+\exp(\frac{r-R_p-R_d+p_2}{p_3})}\right] \text{ MeV}, \tag{5}$$

where the constant coefficients $p_1$, $p_2$ and $p_3$ are equal to -7.65, 1.02 and 0.89, respectively. In Eq. (5), $b$ represents the width of the nuclear surface and was taken to be 1 fm. Moreover, the surface energy coefficients $\gamma$ are obtained as follows,

$$\gamma = 0.9517\left[1 - 1.7826\left(\frac{N-Z}{A}\right)^2\right] \text{MeV.fm}^{-2}, \tag{6}$$

where $N$, $Z$ and $A$ represent the neutron, proton and mass numbers of the parent nucleus, respectively. $R_p$ and $R_d$ can be given by,

$$R_{p(d)} = 1.28A_{p(d)}^{1/3} - 0.76 + 0.8A_{p(d)}^{-1/3} \text{ fm}. \tag{7}$$

In the present study, we use the following equation to calculate the proton radioactivity half-life with the decay constant λ,

$$T_{1/2} = \frac{\ln 2}{\lambda} \tag{8}$$

where $\lambda = \nu P$. Herein, $\nu$ is the assault frequency and can be related to oscillation frequency $\omega$ by:

$$\nu = \frac{\omega}{2\pi} = \frac{2E_\nu}{h} \tag{9}$$

According to Ref. [39], the following law was found for calculating the zero-point vibration energies $E_\nu$ which is proportional to proton radioactivity energy $Q_p$,

$$\begin{aligned} E_\nu &= 0.1045Q_p \text{ for even}(Z)\text{-even}(N) \text{ parent nuclei,} \\ &= 0.0962Q_p \text{ for odd}(Z)\text{-even}(N) \text{ parent nuclei,} \\ &= 0.0907Q_p \text{ for even}(Z)\text{-odd}(N) \text{ parent nuclei,} \\ &= 0.0767Q_p \text{ for odd}(Z)\text{-odd}(N) \text{ parent nuclei.} \end{aligned} \tag{10}$$

In Eq. (9), $h$ denotes the Planck constant. $P$ is the probability of penetration of the potential barrier. It can be obtained in the semi-classical approximation of the WKB by,

$$P = \exp\left[-\frac{2}{\hbar}\int_{r_{\text{in}}}^{r_{\text{out}}}\sqrt{2\mu\left(V_{\text{tot}}(r) - Q_p\right)}dr\right], \tag{11}$$

where the classical turning points $r_{\text{in}}$ and $r_{\text{out}}$ can be satisfied the conditions $V_{\text{tot}}(r_{\text{in}}) = V_{\text{tot}}(r_{\text{out}}) = Q_p$. It is well known that the WKB method is lacking structural information. However, during recent decades, the investigators theoretically studied the one proton radioactivity in the ground state and isomeric state by taking into account various physical effects in half-life calculations, including coupled-channels and deformation effects [40–42]. The obtained results indicate that the mentioned approaches can be applied to the case of proton emission.

## 3. Results and discussion

In the present work, the nuclear proximity model denoted as Zhang 2013 is used to calculate the nuclear part of the interaction potential between the emitted proton and daughter nucleus.

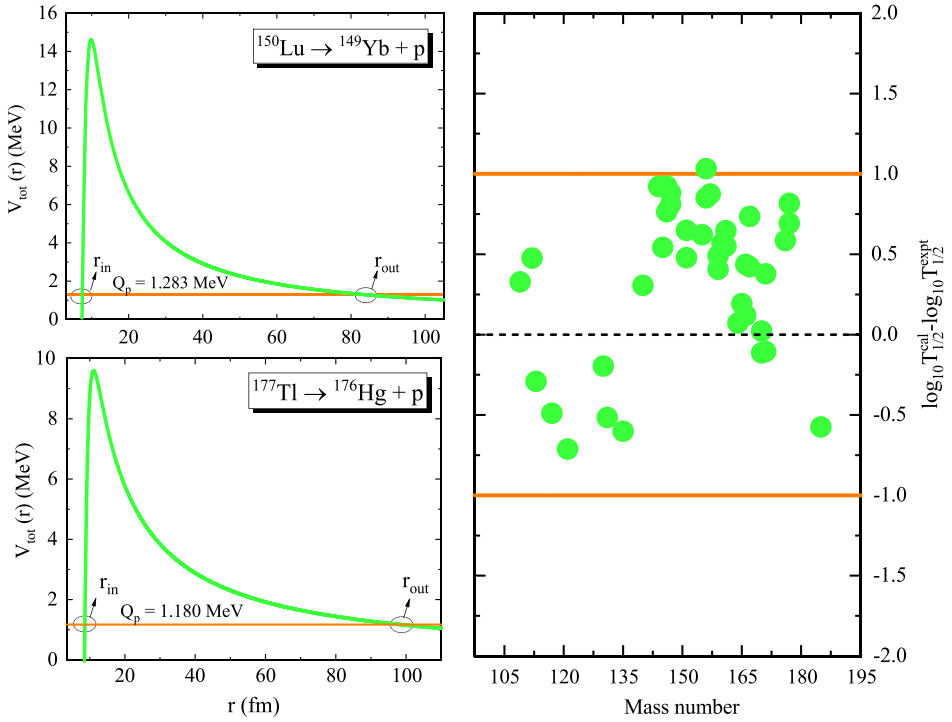


Fig. 1. (Color online.) *Left panel*: The radial behavior of total emitted proton-core interaction potential using the Zhang 2013 proximity potential for $^{150}$Lu and $^{171}$Au decays. The solid orange lines represent the corresponding proton radioactivity energies $Q_p$. *Right panel*: Logarithmic difference of the calculated half-lives with the experimental data as a function of the mass number of 44 experimentally detected proton emitters using the Zhang 2013 proximity potential.

As earlier stated, this version of the proximity formalism was first introduced to study the alpha decay channel of the unstable heavy nuclei [27]. Therefore, it is interesting and important to explore the performance of this model to describe the proton decay mode. In order to access this aim, we calculate the distributions of total emitted proton-core interaction potential for 44 known natural one-proton emitters in the mass region $A = 108 - 185$ corresponding to the charge number $Z = 53 - 83$. The obtained results confirm that the Zhang 2013 formalism is suitable to deal theoretically with the process of proton radioactivity due to the fact the classical turning points $r_{\text{in}}$ can be determined by considering equation $V_{\text{tot}}(r_{\text{in}}) = Q_p$ for different cases of proton radioactivity. In order to verity this conclusion, in the left panels of Fig. 1, we display the total interaction potential $V_{\text{tot}}(r)$ obtained from the proximity potential Zhang 2013 formalism for $^{150}$Lu and $^{171}$Au decays, as two examples. As can be seen from this figure, the classical turning point $r_{\text{in}}$ can be obtained within the framework of the proximity potential Zhang 2013. This means that the depth of the total emitted proton-daughter nucleus interaction potential is below the energy $Q_p$ and therefore the present proximity version is appropriate for dealing with proton radioactivity. It is shown that the estimated values of inner and outer classical turning points are respectively $r_{\text{in}} = 7.52$ fm and $r_{\text{out}} = 84.44$ fm for proton decay from $^{150}$Lu. Further, one can deduce that these values are respectively equal to $r_{\text{in}} = 8.56$ fm and $r_{\text{out}} = 77.61$ fm for proton emitter $^{171}$Au.

To gain further insight, one-proton decay half-lives are calculated using the proximity potentials for all the parent nuclei within the framework of the WKB semiclassical approximation. The obtained results are listed in Table 1. In this table, the first three columns represent the studied parent nuclei, the experimental proton radioactivity energy $Q_p$ and the orbital angular momentum $\ell$ taken away by the emitted protons. Energetically, one can see that the values of decay energy

$$Q_p = \Delta M_p - \left(\Delta M_d + \Delta M_p\right) + k\left(Z_p^{\varepsilon} - Z_d^{\varepsilon}\right) \tag{12}$$

are positive for all the proton emissions and thus the present radioactivity phenomena are possible. In this relation, $\Delta M_p$, $\Delta M_d$ and $\Delta M_p$ are the mass excess of the parent nuclei, daughter nuclei, and the emitted proton, respectively. Note that the term $k(Z_p^{\varepsilon} - Z_d^{\varepsilon})$ represents the screening effect of the atomic electrons [43] with $k = 8.7$ eV, $\varepsilon = 2.517$ for $Z \geq 60$, and $k = 13.6$ eV, $\varepsilon = 2.408$ for $Z < 60$ [44]. The experimental mass excesses are taken from the recent evaluated nuclear properties table NUBASE2020 [45] and the latest evaluated atomic mass table AME2020 [46,47]. The fourth and fifth columns of Table 1 represent the experimental $p$ radioactivity half-lives from ground-states or isomeric states. The calculations by adopting the proximity version Zhang 2013 to evaluate the emitted proton-core interaction potential are listed in the sixth column of Table 1. Now we can determine the differences between calculated and measured half-lives within the framework of the Zhang 2013 model. The results are presented in the right panel of Fig. 1. It can be clearly seen that the values of difference $\log_{10}T_{1/2}^{\text{cal}} - \log_{10}T_{1/2}^{\text{expt}}$ are generally within the range of about $\pm 1$. We obtain the standard deviations between the logarithmic form of the theoretical and experimental values of proton radioactivity half-lives using the following relation,

$$\sigma = \sqrt{\frac{1}{n}\sum_{i=1}^{n}\left[\log_{10}\left(\mathrm{T}_{1/2\mathrm{i}}^{\text{cal}}\right) - \log_{10}\left(\mathrm{T}_{1/2\mathrm{i}}^{\text{expt}}\right)\right]^2}, \tag{13}$$

where $n$ is the number of parent nuclei used for evaluating $\sigma$ values. We can find that the rms deviation deduced from the Zhang 2013 model is $\sigma = 0.740$. This means that the results of the selected model are found to be in good agreement with the half-lives of the experimentally known proton emitters. The fair agreement of our results with experimental values indicates that the Zhang 2013 model can be used to predict half-lives of one-proton emitters. In view of the fact that the orbital angular momentum $\ell$ taken away by the emitted proton plays a vital role in the proton decay process [48,49], we calculate the standard deviations $\sigma$ for different considered cases with the same angular momentums $\ell = 0$ (9-emitters), $\ell = 2$ (15-emitters), $\ell = 3$ (3-emitters), and $\ell = 5$ (17-emitters). The obtained results using the Zhang 2013 analysis for the cases corresponding to $l = 0, 2, 3$ and 5 show that the best values of the standard deviations are found to occur in the cases of $l = 2$.

### *3.1. Sensitivity of the proton-core interaction potential to the temperature effects of parent nuclei*

As discussed in the preceding section, in the studies of the proton radioactivity of nuclei, the nuclear temperature effects can be attributed to the low-lying excitation energies of the 15 certain proton emitters in the isomeric states. Within the framework of the dynamical cluster-decay model for the decay of hot nuclei [50–53], the barrier penetrability for an excited compound system can be expressed as

Table 1
The calculated proton radioactivity half-lives of 44 experimentally detected proton emitters using the Zhang 2013 model. The superscript (m) denotes the isomeric states. The second and third columns are for the experimental released energies [46] and the minimum angular momentum $\ell$. The experimental data proton radioactivity half-lives are taken from [45] with the exception of $T_{1/2}$ for $^{159}$Re and $^{159}$Re$^m$ taken from Ref. [58]. Note that the experimental data of $Q_p$-values for $^{130}$Eu, $^{165}$Ir$^m$, and $^{185}$Bi$^m$ are taken from [58].

| | | | | $\log_{10}T_{1/2}$ (s) | |
|---|---|---|---|---|---|
| Parent nuclei | $Q_p$(MeV) | $\ell_{\min}$ | $T_{1/2}^{\text{expt}}$ | expt | Zhang2013 |
| $^{108}$I | 0.597(13) | 2 | 5.28(222) s | 0.723 | $0.956^{+0.327}_{-0.317}$ |
| $^{109}$I | 0.820(4) | 2 | 92.8(8) μs | -4.032 | $-3.506^{+0.061}_{-0.062}$ |
| $^{112}$Cs | 0.816(4) | 2 | 490(30) μs | -3.310 | $-2.611^{+0.064}_{-0.064}$ |
| $^{113}$Cs | 0.9728(13) | 2 | 16.94(9) μs | -4.771 | $-4.942^{+0.015}_{-0.016}$ |
| $^{117}$La | 0.820(3) | 2 | 21.7(18) ms | -1.664 | $-2.063^{+0.049}_{-0.050}$ |
| $^{121}$Pr | 0.890(10) | 2 | 12(5) ms | -1.921 | $-2.468^{+0.153}_{-0.150}$ |
| $^{130}$Eu | 1.028(15) | 2 | 1.0(4) ms | -3.000 | $-3.002^{+0.198}_{-0.194}$ |
| $^{131}$Eu | 0.947(5) | 2 | 20(3) ms | -1.699 | $-1.985^{+0.075}_{-0.073}$ |
| $^{135}$Tb | 1.188(7) | 3 | 1.01(28) ms | -2.996 | $-3.543^{+0.076}_{-0.076}$ |
| $^{140}$Ho | 1.0939(10) | 3 | 6(3) ms | -2.221 | $-1.762^{+0.012}_{-0.013}$ |
| $^{141}$Ho | 1.177(7) | 3 | 4.1(1) ms | -2.387 | $-2.875^{+0.080}_{-0.079}$ |
| $^{141}$Ho$^m$ | 1.243(7) | 0 | 7.3(3) μs | -5.137 | $-5.324^{+0.073}_{-0.072}$ |
| $^{144}$Tm | 1.712(16) | 5 | 2.3(9) μs | -5.569 | $-4.647^{+0.199}_{-0.088}$ |
| $^{145}$Tm | 1.736(7) | 5 | 3.17(20) μs | -5.499 | $-4.835^{+0.046}_{-0.047}$ |
| $^{146}$Tm | 0.896(6) | 0 | 155(20) ms | -0.810 | $0.093^{+0.106}_{-0.104}$ |
| $^{146}$Tm$^m$ | 1.200(8) | 5 | 73(7) ms | -1.137 | $-0.039^{+0.092}_{-0.094}$ |
| $^{147}$Tm | 1.059(3) | 5 | 3.87(130) s | 0.587 | $1.635^{+0.042}_{-0.041}$ |
| $^{147}$Tm$^m$ | 1.121(6) | 2 | 360(40) μs | -3.444 | $-2.485^{+0.075}_{-0.075}$ |
| $^{150}$Lu | 1.2696(33) | 5 | 45(3) ms | -1.347 | $-0.297^{+0.036}_{-0.036}$ |
| $^{150}$Lu$^m$ | 1.2916(55) | 2 | 40(7) μs | -4.398 | $-3.753^{+0.057}_{-0.057}$ |
| $^{151}$Lu | 1.2392(3) | 5 | 78.4(9) ms | -1.105 | $-0.070^{+0.003}_{-0.007}$ |
| $^{151}$Lu$^m$ | 1.298(4) | 2 | 16.0(5) μs | -4.796 | $-3.929^{+0.041}_{-0.041}$ |
| $^{155}$Ta | 1.453(15) | 5 | 3.2(13) ms | -2.495 | $-1.754^{+0.139}_{-0.137}$ |
| $^{156}$Ta | 1.020(4) | 2 | 149(8) ms | -0.826 | $0.266^{+0.061}_{-0.060}$ |
| $^{156}$Ta$^m$ | 1.114(9) | 5 | 8.57(207) s | 0.933 | $2.119^{+0.123}_{-0.121}$ |
| $^{157}$Ta | 0.935(10) | 0 | 297(106) ms | -0.527 | $0.706^{+0.176}_{-0.172}$ |
| $^{159}$Re | 1.816(20) | 5 | 0.0202(37) ms | -4.694 | $-4.187^{+0.137}_{-0.135}$ |
| $^{159}$Re$^m$ | 1.831(20) | 5 | 21.6(44) μs | -4.665 | $-4.288^{+0.135}_{-0.134}$ |
| $^{160}$Re | 1.267(7) | 2 | 687(11) μs | -3.163 | $-2.382^{+0.079}_{-0.080}$ |
| $^{161}$Re | 1.197(5) | 0 | 440(1) μs | -3.357 | $-2.478^{+0.061}_{-0.062}$ |

Table 1 (*continued*)

| Parent nuclei | $Q_p$(MeV) | $\ell_{\min}$ | $T_{1/2}^{\text{expt}}$ | $\log_{10}T_{1/2}$ (s) | |
|---|---|---|---|---|---|
| | | | | expt | Zhang2013 |
| $^{161}$Re$^m$ | 1.3207(52) | 5 | 210(10) ms | -0.678 | $0.035^{+0.057}_{-0.055}$ |
| $^{165}$Ir$^m$ | 1.717(7) | 5 | 369(38) μs | -3.433 | $-3.087^{+0.053}_{-0.052}$ |
| $^{166}$Ir | 1.152(8) | 2 | 150(72) ms | -0.824 | $-0.391^{+0.108}_{-0.107}$ |
| $^{166}$Ir$^m$ | 1.323(10) | 5 | 839(376) ms | -0.076 | $0.609^{+0.112}_{-0.109}$ |
| $^{167}$Ir | 1.070(4) | 0 | 75.9(2.8) ms | -1.120 | $-0.141^{+0.059}_{-0.060}$ |
| $^{167}$Ir$^m$ | 1.2455(45) | 5 | 6.95(102) s | 0.842 | $1.399^{+0.054}_{-0.054}$ |
| $^{170}$Au | 1.472(12) | 2 | 326(67) μs | -3.487 | $-3.458^{+0.115}_{-0.114}$ |
| $^{170}$Au$^m$ | 1.752(18) | 5 | 1.07(13) ms | -2.971 | $-2.840^{+0.136}_{-0.135}$ |
| $^{171}$Au | 1.448(10) | 0 | 22.3(24) μs | -4.652 | $-4.119^{+0.098}_{-0.097}$ |
| $^{171}$Au$^m$ | 1.703(14) | 5 | 2.59(39) ms | -2.587 | $-2.575^{+0.110}_{-0.109}$ |
| $^{176}$Tl | 1.265(18) | 0 | 6.2(23) ms | -2.208 | $-1.464^{+0.222}_{-0.219}$ |
| $^{177}$Tl | 1.180(20) | 0 | 67(37) ms | -1.174 | $-0.139^{+0.056}_{-0.601}$ |
| $^{177}$Tl$^m$ | 1.963(26) | 5 | 451(106) μs | -3.346 | $-4.050^{+0.172}_{-0.138}$ |
| $^{185}$Bi$^m$ | 1.607(16) | 0 | 64.4(47) μs | -4.191 | $-4.609^{+0.141}_{-0.139}$ |

$$P = \exp\left[-\frac{2}{\hbar}\int_{r_{\text{in}}}^{r_{\text{out}}}\sqrt{2\mu\left(V_{\text{tot}}(r) - Q_{\text{eff}}\right)}dr\right], \tag{14}$$

where $Q_{\text{eff}}$ is the effective $Q$-value given as

$$Q_{\text{eff}} = Q + E^*. \tag{15}$$

On the other hand, the excitation energy of compound system $E^*_{\text{CN}}$ [50–53] related to the nuclear temperature $T$ (in MeV) can be written as

$$E^*_{CN} = \frac{1}{9}AT^2 - T. \tag{16}$$

In heavy ion reactions with enough compound nucleus excitation energy, the relation between the total excitation energy (TXE) and total kinetic energy (TKE) of the decay fragments with $Q_{\text{out}}$ [54] can be written as

$$E^*_{CN} - |Q_{\text{out}}| = TKE(T) - TXE(T), \tag{17}$$

here, $E^*_{CN} = E_{\text{c.m.}} - Q_{in}$ with the $Q$-value of the entrance (incoming) channel. Note that the experimental excitation energies $E^*$ for the available proton emitters are extracted from Refs. [45,46]. The calculated results have been tabulated in the third column of Table 2. We can find that the calculated nuclear temperatures $T$ for different proton decay processes are ranged from $T = 0.387$ to 0.483 MeV. Here, we are interested in analyzing the behavior of these values as a function of the mass number of the parent nuclei, see Fig. 2. From this figure, one can find that the nuclear temperatures have generally an increasing trend with mass number $A_p$. Although, a little variation in the mass of nuclei existed with temperature.

Table 2
The comparison of the calculated half-lives of the proton emitters in the isomeric state using the original and modified forms of the Zhang 2013 model with the corresponding experimental data. The superscript (m) denotes the isomeric states. The calculated values of the nuclear temperature $T$ of hot proton emitters have been listed.

| Parent nuclei | $\ell$ | $T$ | $\log_{10}T_{1/2}$ (s) | | | |
|---|---|---|---|---|---|---|
| | | (MeV) | expt | Zhang2013 | Zhang2013(TD)[a] | Zhang2013(TD)[b] |
| $^{141}$Ho$^{m}$ | 0 | 0.430 | -5.137 | -5.324 | $-5.602^{+0.073}_{-0.074}$ | $-5.288^{+0.072}_{-0.073}$ |
| $^{146}$Tm$^{m}$ | 5 | 0.416 | -1.137 | -0.039 | $-0.495^{+0.093}_{-0.093}$ | $0.024^{+0.093}_{-0.091}$ |
| $^{147}$Tm$^{m}$ | 2 | 0.401 | -3.444 | -2.485 | $-2.785^{+0.076}_{-0.075}$ | $-2.446^{+0.075}_{-0.075}$ |
| $^{150}$Lu$^{m}$ | 2 | 0.424 | -4.398 | -3.753 | $-4.069^{+0.057}_{-0.058}$ | $-3.712^{+0.057}_{-0.057}$ |
| $^{151}$Lu$^{m}$ | 2 | 0.423 | -4.796 | -3.393 | $-4.244^{+0.041}_{-0.042}$ | $-3.888^{+0.041}_{-0.041}$ |
| $^{156}$Ta$^{m}$ | 5 | 0.387 | 0.933 | 2.120 | $1.690^{+0.125}_{-0.122}$ | $2.180^{+0.124}_{-0.122}$ |
| $^{159}$Re$^{m}$ | 5 | 0.483 | -4.665 | -4.187 | $-4.796^{+0.138}_{-0.135}$ | $-4.215^{+0.134}_{-0.134}$ |
| $^{161}$Re$^{m}$ | 5 | 0.412 | -0.678 | 0.035 | $-0.412^{+0.056}_{-0.059}$ | $-0.099^{+0.255}_{-0.142}$ |
| $^{165}$Ir$^{m}$ | 5 | 0.460 | -3.433 | -3.087 | $-3.573^{+0.052}_{-0.054}$ | $-3.017^{+0.053}_{-0.052}$ |
| $^{166}$Ir$^{m}$ | 5 | 0.406 | -0.076 | 0.609 | $0.166^{+0.113}_{-0.112}$ | $0.671^{+0.112}_{-0.109}$ |
| $^{167}$Ir$^{m}$ | 5 | 0.393 | 0.842 | 1.399 | $0.967^{+0.056}_{-0.054}$ | $1.456^{+0.057}_{-0.051}$ |
| $^{170}$Au$^{m}$ | 5 | 0.457 | -2.971 | -2.840 | $-3.325^{+0.138}_{-0.136}$ | $-2.771^{+0.135}_{-0.134}$ |
| $^{171}$Au$^{m}$ | 5 | 0.449 | -2.587 | -2.575 | $-3.052^{+0.111}_{-0.112}$ | $-2.507^{+0.110}_{-0.109}$ |
| $^{177}$Tl$^{m}$ | 5 | 0.472 | -3.346 | -4.050 | $-4.542^{+0.173}_{-0.171}$ | $-3.980^{+0.171}_{-0.167}$ |
| $^{185}$Bi$^{m}$ | 0 | 0.419 | -4.191 | -4.609 | $-4.904^{+0.142}_{-0.141}$ | $-4.570^{+0.180}_{-0.100}$ |

[a] Present TD form of $\gamma(T)$, Eq. (19).
[b] Present TD form of $\gamma(T)$, Eq. (1).

During recent years, the modified TD forms of the various parameters of the proximity-type potentials such as the effective sharp radius [55], the surface width [56] and the surface energy coefficient [30] have been introduced to study the thermal behavior of the alpha decay process of hot parent nuclei. We note that these parameters allow us to analyze the effect of the temperature dependence of the effective potential, the quantum tunneling process through the decay barrier and thus $\alpha$-decay half-lives [30,31,57]. Similarly, the process of proton radioactivity may be also depends on the thermal effects of hot parent nuclei. Therefore, the analysis of the effects of temperature dependence on the effective nucleus-nucleus potential and also proton radioactivity half-lives $T_{1/2}$ can be an interesting topic for proton emitters in the isomeric states. In this work, we try to investigate the hot proton emitters by integrating temperature effects on the nuclear surface tension coefficient $\gamma$ of the proximity potential Zhang 2013 formalism within the framework of the finite-temperature generalized liquid-drop model [59]. In order to assess this purpose, we introduce a modified form of the $\gamma$ coefficient as follows

$$\gamma\,(T) = \gamma\,(T=0)\left[1 + aT\right]^{b}\ \mathrm{MeV.fm}^{-2}. \tag{18}$$

where $\gamma(T=0)$ is the temperature-independent (T-IND) form of the surface energy coefficient as calculated by Eq. (6). In addition, in Eq. (18), the two constants $a$ and $b$ can be determined

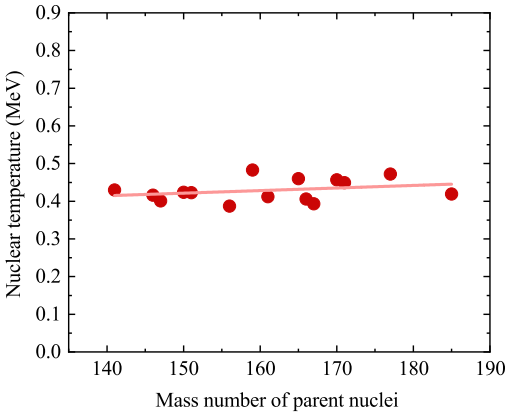


Fig. 2. (Color online.) The variation of the calculated nuclear temperatures as a function of the mass number of the parent hot nuclei.

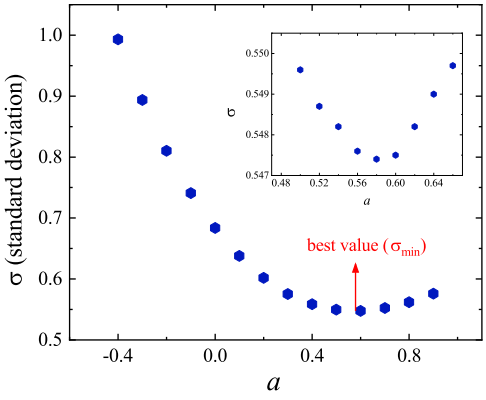


Fig. 3. (Color online.) The dependence of the calculated values of the standard deviation $\sigma$ on the values of the coefficient $a$ in the suggested Eq. (18). The best value of $\sigma$ is obtained for $a = 0.58$.

through fitting to the experimental half-lives of all parent nuclei in the isomeric states. The calculated results reveal that the best standard deviation is found to occur at $a = 0.58$ and $b = 2$. To obtain further insight into this problem, we display a set of results in Fig. 3. In this figure, the coefficient $a$ is varied from -0.4 to 0.90, whereas the exponent $b$ is fixed at $b = 2$. The relationship between the $\sigma$ and $a$ demonstrates that the standard deviation between the measured and calculated values of the proton radioactivity half-lives is smallest when $a$ is equal to 0.58.

Taking into account all above, we develop a new modified form of the surface tension coefficient $\gamma$ for considering the effect of nuclear temperature in the process of proton radioactivity as,

$$\gamma\,(T) = \gamma\,(T=0)\Big[1 + 0.58T\Big]^2 \ \mathrm{MeV.fm^{-2}}. \tag{19}$$

By imposing the proposed formula in the Zhang 2013 model, we obtain a modified form of the proximity potential as “Zhang 2013(TD)”. Note that in the case of hot nuclei in addition to

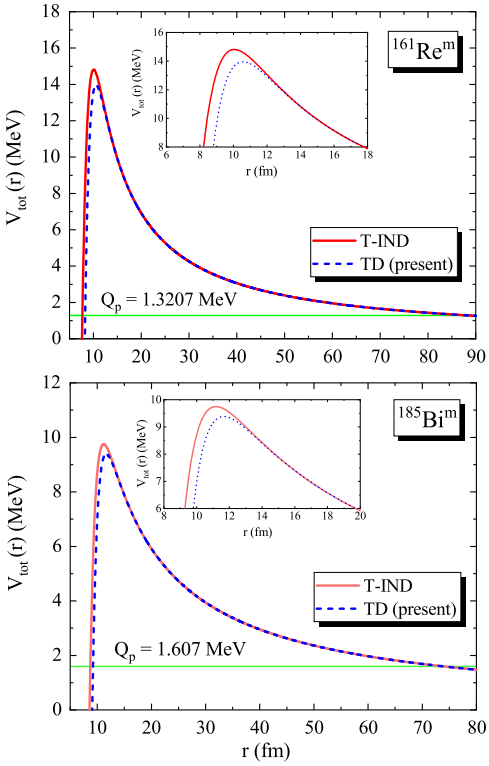


Fig. 4. (Color online.) The radial behavior of total interaction potential $V_{\rm tot}$ (in MeV) using T-IND and TD forms of the Zhang 2013 model for proton decay process of $^{161}$Re$^{\rm m}$ and $^{185}$Bi$^{\rm m}$ nuclei.

surface energy coefficient, the radius $R_{p(d)}$ and surface width $b$ parameters [60] are temperature dependent as follows

$$R_i(T) = R_i(T=0)[1+0.0007T^2], \tag{20}$$

$$b(T) = b(T=0)[1+0.009T^2]. \tag{21}$$

So, in the present study, the effect of nuclear temperature $T$ is included via all three parameters $\gamma(T)$, $R_i(T)$, and $b(T)$. Although it is clear from Eqs. (19) to (21) that the influence of TD form of the surface energy coefficient on the nucleus-nucleus potential is far more than two other coefficients. In order to quantitative analyze the role of nuclear temperature in the radial distribution of the total emitted proton-daughter nucleus interaction potentials $V_{\rm tot}$, in Fig. 4, we display these potentials based on the T-IND and TD forms of the Zhang 2013 model for proton decay process of $^{161}$Re$^{\rm m}$ and $^{185}$Bi$^{\rm m}$ nuclei, as two examples. The short dashed line in each panel of this figure denotes the characteristic quantity $Q_p$-value. One can see that the usage of the present TD pattern leads to decrease the height and width of the Coulomb barrier between the emitted proton and the daughter nucleus. The reason can be mainly attributed to the strength of the surface energy coefficients calculated by the original and modified forms of the Zhang 2013 model. We can clearly see that the new parameterized formula (19) provides the larger values for this coefficient in comparison with the original formula (6). For $^{161}$Re$^{\rm m}$ and $^{185}$Bi$^{\rm m}$ decays, the calculated surface energy coefficients are $\gamma^{\rm TD(T-IND)}$=1.44957(0.94378) MeV.fm$^{-2}$

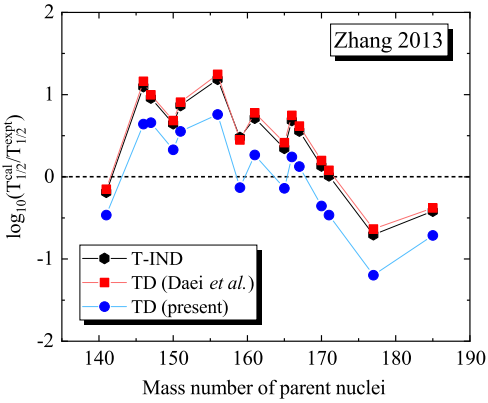


Fig. 5. (Color online.) Logarithmic difference of calculated half-lives with the corresponding experimental data as a function of the mass number of 15 proton emitters in the isomeric state. The calculated values correspond to the results of the Zhang 2013 model and its modified form with Eqs. (1) and (19).

and $\gamma^{\mathrm{TD(T-IND)}}$=1.44411(0.93380) MeV.fm$^{-2}$, respectively. On the other hand, as shown in Eq. (5) the nuclear proximity potential depends directly on the surface energy coefficient. Therefore, it can be concluded that the interaction potentials calculated by the original version of the Zhang 2013 model will be less attractive compared to its TD form.

### 3.2. *Sensitivity of the proton radioactivity half-lives to the temperature effects of parent nuclei*

In order to further test the quality of the presently obtained formula $\gamma(T)$, using Eq. (19), we calculate the logarithmic theoretical proton radioactivity half-life $\log_{10}T^{\mathrm{cal}}_{1/2}$ based on the proximity potential Zhang 2013(TD) formalism. The calculated results are compared with the experimental data and those obtained by the original proximity potential Zhang 2013 in Table 2. Herein, we also use the modified TD surface energy coefficient (19), radius (20), and surface width (21) for incorporating the temperature dependence on the total proton-core interaction potential and resulting in the proton radioactivity half-lives. The calculated proton radioactivity half-lives have been presented in the sixth column of Table 2. In Fig. 5, we plot the decimal logarithm deviations between the experimental data of proton radioactivity half-lives and those obtained by the T-IND and TD forms of the Zhang 2013 model as a function of the mass number of the proton emitters in the isomeric states. After imposing the thermal effects of the surface energy coefficient using Eq. (19), we can find the calculated difference $\log T^{\mathrm{cal}}_{1/2}-\log T^{\mathrm{expt}}_{1/2}$ is mainly around zero. In fact, compared to the original proximity potential Zhang 2013, one can see that the agreement with the experimental data improves by $\frac{0.686-0.548}{0.686}=20\%$ by considering the present temperature dependence pattern in the proximity formalism. Under these conditions, the presently modified form of the proximity potential can be adopted to obtain the precise calculations of proton radioactivity half-lives for proton emitters in the isomeric states. While, Fig. 5 shows that by including the temperature dependence in the proximity formalism through Eq. (1) instead of Eq. (19), the agreement with the experimental half-lives is reduced by more than 4%. As a result of the literature analysis, other physical factors can also be exist that cause the discrepancy between theoretical and experimental values of $\alpha$ half-lives. The spectroscopic factor $S$ may be considered as the overlap of the actual ground-state configuration and the configuration representing the proton coupled to the ground state of the daughter. Obviously, its value

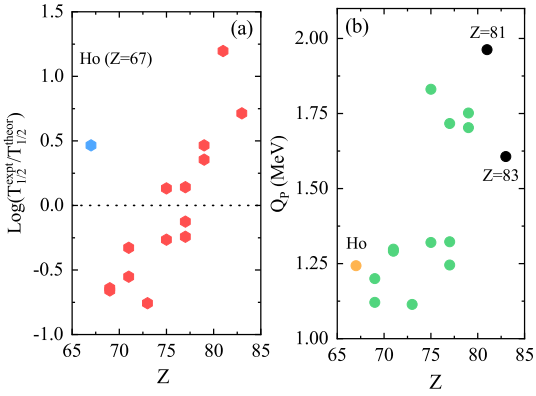


Fig. 6. (Color online.) (a) Deviations between the calculated half-lives and the measured values as a function of the charge number $Z$ of proton emitters using the Zhang 3013 (TD) model. (b) Dependence of the $Q_p$-values upon the atomic number $Z$ of 15 proton emitters in the isomeric state.

is expected to be less than unity. When spectroscopic factor $S$ is included the half-life value will be higher than the predicted values without including spectroscopic factor. The inclusion of ground state deformation reduces the height and width of the barrier as a result penetrability will increase. In this situation, one can conclude that the theoretical half-lives decrease [61,62].

We also notic from Fig. 5 that the sudden changes appear in the $\log_{10}(T_{1/2}^{\rm cal}/T_{1/2}^{\rm expt})$ values around $^{141}_{67}\mathrm{Ho}^{m}$ and between the special cases $^{177}_{81}\mathrm{Te}^{m}$ and $^{185}_{83}\mathrm{Bi}^{m}$. To obtain further insight into these changes, we plot in Fig. 6(a) the comparison of the calculated half-lives with the corresponding experimental data as a function of the atomic number $Z$ of all 15 proton emitters using the TD form of the Zhang 2013 model. One can see that a pronounced change occurs at the proton drip line between $Z = 67$ and $Z = 69$. Similar behaviors were previously reached in Refs. [20,63,64]. As seen in Fig. 6(b), one cannot provide a satisfactory description of this sudden change by plotting the $Q_p$-values as a function of $Z$. In this situation, the physical justification for the observed phenomenon may be attributed to an abrubt shape change occurring at around $Z = 68$ [63,64]. The results shown in Fig. 6(a) also confirm the occurrence of a sudden change between the $Z = 81$ and $Z = 83$. This phenomenon due to the strong shell effect may be caused by an abrupt change in the $Q_p$-values, see Fig. 6(b).

### *3.3. Prediction of the half-lives of the proton emitters*

The agreement attained in reproducing the experimental data of proton emitters in the isomeric state allows us to predict the proton radioactivity half-lives of 6 nuclei in region $Z = 57 - 83$ using the modified Zhang 2013 model. We note that for these nuclei the proton radioactivity is energetically allowed but not verified yet experimentally. The results are reported in Table 3. The first four columns of this table denote the parent nucleus, the calculated temperature, the corresponding decay energy $Q_p$, and the angular momentum taken away by the proton particle, respectively. The next two columns show logarithmic half-lives $\log_{10}T_{1/2}$ of the experimental data and the Zhang 2013 (TD) model, respectively. The seventh and eighth columns present for comparison the results of the new Geiger-Nuttall law (NGNL) from Chen et al. [49] and the universal decay law for proton emission (UDLP) from Qi et al. [19], respectively. On analyzing the table, it is found that the predicted proton radioactivity half-lives using the present approach

Table 3
A comparison of predicted proton radioactivity half-lives of 6 hot parent nuclei in the region $Z = 57 - 83$ using the modified form of the Zhang 2013 model and those obtained by NGNL and UDLP approaches. The superscript (m) denotes the isomeric states.

| Parent nuclei | $T$ | $Q_p$ | $\ell$ | $\log_{10}T_{1/2}$ (s) | | | | |
|---|---|---|---|---|---|---|---|---|
| | (MeV) | (MeV) | | expt | Zhang2013(TD) | NGNL | UDLP | Our formula (24) |
| $^{117}$La$^{m}$ | 0.422 | 0.951 | 4 | $\approx -1.989$ | -2.185 | -2.094 | -2.155 | -3.549 |
| $^{146}$Tm$^{n}$ | 0.406 | 1.144 | 5 | – | 0.227 | -0.205 | -0.176 | -0.896 |
| $^{169}$Ir$^{m}$ | 0.315 | 0.780 | 5 | – | 8.373 | 8.088 | 7.404 | 7.202 |
| $^{171}$Ir$^{m}$ | 0.233 | 0.402 | 5 | – | 13.048 | 21.952 | 20.396 | 17.426 |
| $^{172}$Au$^{m}$ | 0.283 | 0.627 | 2 | $> -0.260$ | 8.349 | 9.678 | 9.448 | 5.574 |
| $^{185}$Bi$^{n}$ | 0.433 | 1.720 | 6 | – | -1.011 | -1.504 | -1.161 | -0.940 |

are all within the range of the experimental data. In addition, the comparison results indicate that the half-lives predicted using our method for different proton emitters are given in the same order with the NGNL and UDLP approaches except for $^{171}$Ir$^{m}$.

### 3.4. Improved empirical formula for the one-proton transition from isomeric states

The first empirical linear equation between the alpha decay half-lives and the decay energy $Q_\alpha$ of the emitted alpha particle was found by Geiger and Nuttall [65]. Thereafter, several researchers have been proposed the empirical formulas for calculating the half-lives of alpha decay, see for example Refs. [66–68]. In 2006, similar to the Geiger-Nuttall law, Delion et al. [64] first suggested a simple empirical formula for proton radioactivity half-lives in the physical process of one-proton decay. In another attempt, Sreeja et al. [48] proposed a new model-independent formula by considering the dependence on the angular momentum $\ell$ carried by the proton. Recently, Chen et al. [49] suggested a two-parameter formula for proton radioactivity half-life with including the contributions of the charge of the daughter nucleus and the orbital angular momentum taken away by the emitted proton.

It would be of interest to discuss the thermal behavior of the logarithm of the experimental proton radioactivity half-lives of the proton emitters in the isomeric state. To reach this goal, in Fig. 7, we analyze the relationships between the logarithm of the experimental half-life and $\xi = \frac{Z_d^\beta}{\sqrt{T}}$, inspired by the ratio of $\frac{Z_d^{0.8}}{\sqrt{Q}}$ in the new Geiger-Nuttall rules [49]. Note that the calculated values of the temperature $T$ (in MeV) are taken from the second column of Table 2 for all 15 experimentally detected proton emitters. As a result of the literature [29,48,49], one can find that the proton decay half-lives are very sensitive to the orbital angular momentum $\ell$ associated with the transitions. Therefore, in this figure the variation of the experimental data of the logarithm of the half-life against $\xi$ has been separately plotted for different $\ell$-values, namely $\ell = 0$ (2-emitters), $\ell = 2$ (3-emitters) and $\ell = 5$ (10-emitters). Our primary analysis shows that the experimental trend of half-life values has a large scatter for the proton emitters with $l = 5$ for the exponent of $\beta = 0.7$ and 0.8. We therefore used the lower exponent values of $\beta$ (= 0.0, 0.1, 0.2 and 0.3) in the $Z_d$ term. As can be seen from Fig. 7, the experimental data for proton emitters corresponding to the different angular momentum $\ell = 0$, 2 and 5 follow an increasing linear trend with $\xi$. However, our comparisons in this figure show that the scattering of data is

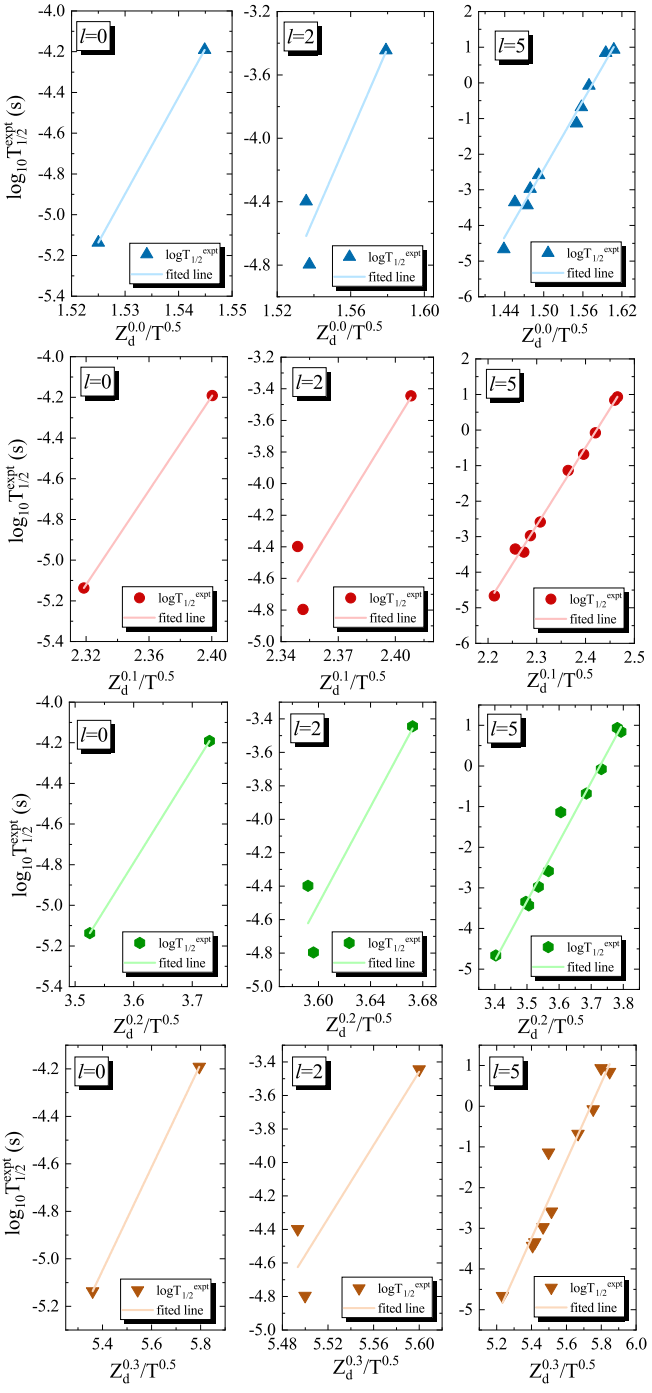


Fig. 7. (Color online.) The logarithm of the experimental half-life of proton emitters with $\ell = 0$, 2 and 5 as a function of the $\xi = \frac{Z_d^{\beta}}{\sqrt{T}}$. Notice that the results are plotted for $\beta = 0$ and 0.1.

Table 4
The extracted values of the slope $a$ and intercept $b$ for different values of $\ell$ (=0, 2, and 5) and $\beta$ (=0.1, 0.2, and 0.3).

| | $\beta = 0.0$ | | $\beta = 0.1$ | | $\beta = 0.2$ | | $\beta = 0.3$ | |
|---|---|---|---|---|---|---|---|---|
| $\ell$ | $a$ | $b$ | $a$ | $b$ | $a$ | $b$ | $a$ | $b$ |
| 0 | 47.56(0.0) | -77.67(0.0) | 11.56(0.0) | -31.95(0.0) | 4.62(0.0) | -21.45(0.0) | 2.17(0.0) | -16.78(0.0) |
| 2 | 26.77(9.09) | -45.74(14.10) | 19.58(6.74) | -50.62(15.99) | 14.52(5.09) | -56.78(18.45) | 10.95(3.93) | -64.82(21.77) |
| 5 | 31.82(1.47) | -50.14(2.24) | 21.84(0.52) | -52.92(1.23) | 14.64(0.69) | -54.60(2.50) | 9.53(0.85) | -54.74(4.67) |

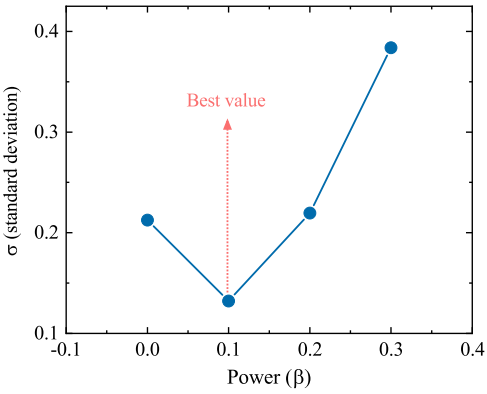


Fig. 8. (Color online.) The dependence of the calculated values of the standard deviation $\sigma$ on the values of the power $\beta$ in the suggested Eq. (22). The best value of $\sigma$ is obtained for $\beta = 0.1$.

increased with increase of the exponent is varied from 0 to 0.3. One can formulate the observed trends using the least square fit as follows,

$$\log_{10} T_{1/2} = a_\ell \left( \frac{Z_d^\beta}{\sqrt{T}} \right) + b_\ell, \tag{22}$$

where the values of slope $a_\ell$ and intercept $b_\ell$ are listed in Table 4 for different values of $\ell$ and $\beta$. To select the best value for the exponent $\beta$ in $Z_d^\beta$ term, we calculate the standard deviation $\sigma$ of the calculations from empirical formula (22) with respect to the corresponding experimental data for different values of $\ell$. The dependence of the calculated values of $\sigma$ on the exponent of $\beta$ has been shown in Fig. 8. From this figure, one can see that the choice of power $\beta = 0.1$ gives the best standard deviation ($\sigma = 0.1322$). On the other hand, one can see from Table 4 that the above formula involves six parameters for the use of each of the exponent values of $\beta$. In order to reduce the number of parameters and also generalize the formula presented in Eq. (22) for predicting half-lives of proton emitters with $l$-values other than $\ell = 0$, 2 and 5, we try to analyze the variation of the slopes $a_\ell$ and the corresponding intercepts $b_\ell$ as a function of angular momentum $\ell$. The results have been shown in Fig. 9. From this figure, we can find that a linear dependence of the slopes and intercepts as a function of angular momentum $\ell$ is obvious when the exponent $\beta$ on $Z_d$ is taken as 0.1. Such dependencies can be interpreted in terms of the $\ell$-dependent functions for the slopes and intercepts values as follows

$$\begin{cases} a(\ell) = 1.9531 \times \ell + 13.1026 \\ b(\ell) = -3.9234 \times \ell - 36.0086 \end{cases} \tag{23}$$

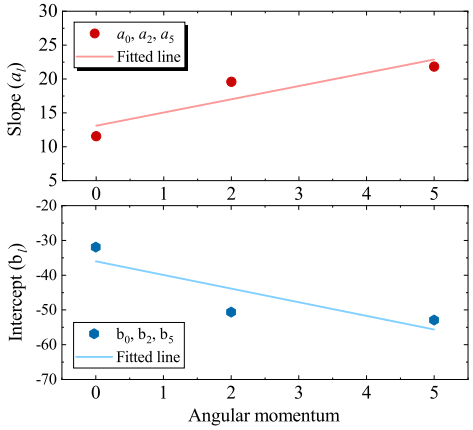


Fig. 9. (Color online.) The variation of the slopes $a_\ell$ and intercepts $b_\ell$ obtained corresponding to $\ell = 0, 2$ and 5 as a function of the angular momentum $\ell$. In each panel, the fitted line is displayed by solid line.

By substituting these functions in Eq. (22), we can propose a final empirical formula for proton radioactivity half-life by keeping the exponent of the $Z_d$ as 0.1. This formula can be written as

$$\log_{10} T_{1/2} = (a \times \ell + b)\left(\frac{Z_d^{0.1}}{\sqrt{T}}\right) + (c \times \ell + d), \tag{24}$$

where $a = 1.9531$, $b = 13.1026$, $c = -3.9234$ and $d = -36.0086$. Now, our empirical formula involves four parameters. It is interesting to investigate the validity of the presently obtained formula for the half-lives of isomeric state one proton emission in reproducing the corresponding experimental data. In Table 5, a numerical comparison is performed between the calculated logarithmic half-lives using Eq. (24) and those obtained by two previous empirical formulas [48,49] for 15 experimentally detected one-proton transitions from isomeric state. Here, we marked these formulas as SBF 2018 [48] and NGNL [49]. It must be noted that these empirical formulas like the Geiger-Nuttal law are parameterized as a function of the inverse square root of the $Q_p$-values. To gain further insight into the validity of the analytical formula (24), we calculate the standard deviation $\sigma$ of the three empirical estimates with respect to the experimental data. The obtained results reveal that our new formula ($\sigma = 0.444$) in comparison with the SBF 2018 ($\sigma = 0.536$) and NGNL ($\sigma = 0.575$) can better reproduce the experimental data. It means that the $T$-dependence can be appropriate for the half-life estimates for the one-proton transition from isomeric states. Herein, we would like to apply our analytical formula (24) for predicting the proton radioactivity half-lives of 6 cases $^{117}$La$^{m}$, $^{146}$Tm$^{n}$, $^{169}$Ir$^{m}$, $^{171}$Ir$^{m}$, $^{172}$Au$^{m}$ and $^{185}$Bi$^{n}$. The obtained results are tabulated in the last column of Table 3. One can see from this table that the half-life information predicted by our method are all within the range of $\log_{10} T_{1/2}^{\text{expt}}$. However, a large difference is seen between our results and those obtained by NGNL and UDLP approaches for two cases $^{171}$Ir$^{m}$ and $^{172}$Au$^{m}$.

## 4. Conclusions

To summarize, the influence of temperature dependence of the proton-core interaction potential through the nuclear surface tension coefficient $\gamma$ on the half-lives of proton decay processes is investigated for 15 experimental data of proton emitters in the isomeric state. The calculations

Table 5
Comparison of the calculated proton radioactivity half-lives of the studied proton emitters in the excited isomeric states with different theoretical methods and experimental values. The calculations of $\log_{10}T_{1/2}$ are performed by using the present empirical formula (24), SBF 2018 [48] and NGNL [49]. Elements with upper suffixes 'm' indicate assignments to excited states.

| Parent nuclei | $\ell$ | $T$ | $\log_{10}T_{1/2}$ (s) | | | |
|---|---|---|---|---|---|---|
| | | (MeV) | expt | Eq. (24) | SBF 2018 | NGNL |
| $^{141}$Ho$^{m}$ | 0 | 0.430 | -5.137 | -5.629 | -5.470 | -5.605 |
| $^{185}$Bi$^{m}$ | 0 | 0.419 | -4.191 | -4.557 | -4.498 | -4.606 |
| $^{147}$Tm$^{m}$ | 2 | 0.401 | -3.444 | -2.896 | -2.348 | -2.318 |
| $^{150}$Lu$^{m}$ | 2 | 0.423 | -4.796 | -3.859 | -3.542 | -3.569 |
| $^{151}$Lu$^{m}$ | 2 | 0.424 | -4.398 | -3.906 | -3.485 | -3.511 |
| $^{146}$Tm$^{m}$ | 5 | 0.416 | -1.137 | -1.558 | -1.045 | -0.843 |
| $^{156}$Ta$^{m}$ | 5 | 0.387 | 0.933 | 0.752 | 1.218 | 1.247 |
| $^{159}$Re$^{m}$ | 5 | 0.483 | $-4.665$[c] | -5.022 | -4.550 | -4.586 |
| $^{161}$Re$^{m}$ | 5 | 0.412 | -0.678 | -0.835 | -0.524 | -0.574 |
| $^{165}$Ir$^{m}$ | 5 | 0.460 | -3.433 | -3.634 | -3.304 | -3.413 |
| $^{166}$Ir$^{m}$ | 5 | 0.406 | -0.076 | -0.284 | 0.028 | -0.103 |
| $^{167}$Ir$^{m}$ | 5 | 0.393 | 0.842 | 0.623 | 0.864 | 0.726 |
| $^{170}$Au$^{m}$ | 5 | 0.457 | -2.971 | -3.328 | -3.046 | -3.225 |
| $^{171}$Au$^{m}$ | 5 | 0.449 | -2.587 | -2.864 | -2.701 | -2.882 |
| $^{177}$Tl$^{m}$ | 5 | 0.472 | -3.346 | -5.022 | -4.550 | -4.586 |

[c] Taken from Ref. [58].

of the interaction potential have been performed using the Zhang 2013 model. The proton radioactivity is processed by the WKB method. The main conclusions of the present paper can be summarized as follows.

- In the first step, we would like to test the validity of the proximity potential Zhang 2013 formalism for studying the proton emission process from neutron-deficient nuclei lying near the proton drip line. In order to reach this goal, we have calculated the total emitted proton-core interaction potentials and also the proton radioactivity half-lives for the 44 experimentally known proton emitters in the ground state and isomeric states. The obtained results show that the logarithmic values of $T_{1/2}^{\text{Zhang2013}}$ can well reproduce the corresponding experimental data. This means that the present proximity potential is convenient to study the one-proton decay processes.
- Analogous to the thermal properties of liquids and hot nuclei, we introduced a TD form of the surface energy coefficient used in nuclear proximity potential within the framework of the finite-temperature generalized liquid-drop model. By imposing this modified form of the coefficient $\gamma(T)$ in the proximity potential Zhang 2013 formalism, one can conclude that the agreement between the experimental data and the calculated values of proton radioactivity half-lives significantly improves by 20% for the known hot proton emitters.
- Our calculated values for the logarithm of the half-life are compared with the available TD approaches. Further, we have extended the proposed TD form of the proximity potential Zhang 2013 to predict the proton radioactivity half-lives of 6 protons emitter in the isomeric

state, whose proton radioactivity is energetically allowed or observed but not yet quantified. It is demonstrated that our predictions are found to be in good agreement with the predictions performed using the other theoretical methods, namely UDLP and NGNL.

- By analyzing the experimental trend of half-life values for proton transitions from isomeric states as a function of the inverse square root of the nuclear temperature $T$, for the first time, we put forwarded a TD empirical formula with only four parameters for estimating the logarithm of half-lives of proton radioactivity. In fact, it is the relation of logarithmic values of the proton radioactivity half-life $\log_{10}T_{1/2}$, nuclear temperature $T$, the charge of the daughter nucleus $Z_d$ and orbital angular momentum $\ell$.
- The obtained results revel that the predictions caused by our model independent formula fairly agree with the experimental data of 15 cases in the excited or isomeric state transition. The fair agreement of our results with experimental values indicate that the presently obtained formula can be used to predict half-lives of new proton emitters and also for further experimental and theoretical research.
- In the preset study, we have compared the results of the empirical formula presented in Eq. (24) with other model predictions of Refs. [48,49]. It is shown that the predictions of this formula are found to be in better agreement with the experimental data for the proton emitters in the isomeric states than the SBF 2019 and NGNL. This result indicates that the temperature dependence can be appropriate for estimating the half-life of proton radioactivity in the excited states.

## CRediT authorship contribution statement

**R. Gharaei:** Conceptualization, Data curation, Methodology, Supervision, Validation, Writing – review & editing. **M. Jalali Shakib:** Formal analysis, Investigation, Methodology, Software, Validation. **K.P. Santhosh:** Conceptualization, Validation, Writing – review & editing.

## Declaration of competing interest

The authors declare that they have no known competing financial interests or personal relationships that could have appeared to influence the work reported in this paper.

## Data availability

The datasets generated during and/or analyzed during the current study are available from the corresponding author on reasonable request.

## References

[1] S. Hofmann, P. Armbruster, W. Faust, K. Guttner, F.P. Hessberger, G. Münzenberg, W. Reisdorf, J.H.R. Schneider, B. Thuma, in: 4th Int. Conf. on Nuclei Far from Stability, Geneva, CERN 81-09, 1981, pp. 190–201.
[2] M. Pfützner, M. Karny, L.V. Grigorenko, K. Riisager, Rev. Mod. Phys. 84 (2012) 567.
[3] S. Hoffman, Nuclear Decay Modes. Chapter 3. Proton Radioactivity, Institute of Physics Publishing, 1996, pp. 143–203.
[4] K.P. Jackson, C.U. Cardinal, H.C. Evans, N.A. Jelley, J. Cerny, Phys. Lett. B 33 (1970) 281.
[5] J. Cerny, J. Esterl, R.A. Gough, R.G. Sextro, Phys. Lett. B 33 (1970) 284.
[6] M. Karnys, K.P. Rykaczewski, R.K. Grzywacz, et al., Phys. Lett. B 664 (2008) 52.
[7] J.M. Dong, H.F. Zhang, G. Royer, Phys. Rev. C 79 (2009) 054330.
[8] M. Bhattacharya, G. Gangopadhyay, Phys. Lett. B 651 (2007) 263.

[9] Y.B. Qian, Z.Z. Ren, D.D. Ni, Chin. Phys. Lett. 27 (2010) 072301.
[10] J.G. Deng, X.H. Li, J.L. Chen, J.H. Cheng, X.J. Wu, Eur. Phys. J. A 55 (2019) 58.
[11] H.F. Zhang, J.M. Dong, Y.Z. Wang, et al., Chin. Phys. Lett. 26 (2009) 072301.
[12] Y. Qian, Z. Ren, Eur. Phys. J. A 52 (2016) 68.
[13] K.P. Santhosh, I. Sukumaran, Eur. Phys. J. A 54 (2018) 102.
[14] G. Gamow, Z. Phys. 51 (1928) 204.
[15] X.J. Bao, H.F. Zhang, H.F. Zhang, G. Royer, J.Q. Li, Nucl. Phys. A 921 (2014) 85.
[16] B. Buck, A.C. Merchant, S.M. Perez, Phys. Rev. C 45 (1992) 1688.
[17] S. Aberg, P.B. Semmes, W. Nazarewicz, Phys. Rev. C 56 (1997) 1762.
[18] D.N. Basu, P. Roy Chowdhury, C. Samanta, Phys. Rev. C 72 (2005) 051601(R).
[19] C. Qi, D.S. Delion, R.J. Liotta, et al., Phys. Rev. C 85 (2012) 011303(R).
[20] Y. Qian, Z. Ren, Eur. Phys. J. A 52 (2016) 68.
[21] M. Balasubramaniam, N. Arunachalam, Phys. Rev. C 71 (2005) 014603.
[22] J.M. Dong, H.F. Zhang, Y.Z. Wang, W. Zuo, J.Q. Li, Nucl. Phys. A 832 (2010) 198.
[23] J. Blocki, J. Randrup, W.J. Swiatecki, C.F. Tsang, Ann. Phys. 105 (1977) 427.
[24] R. Gharaeia, S. Mohammadi, Eur. Phys. J. A 55 (2019) 119.
[25] O.N. Ghodsi, A. Daei-Ataollah, Phys. Rev. C 93 (2016) 024612.
[26] K.P. Santhosha, Indu Sukumaran, Eur. Phys. J. A 53 (2017) 246.
[27] G.L. Zhang, H.B. Zheng, W.W. Qu, Eur. Phys. J. A 49 (2013) 10.
[28] C. Guo, G. Zhang, X. Le, Nucl. Phys. A 897 (2013) 54.
[29] K.P. Santhosh, I. Sukumaran, Phys. Rev. C 96 (2017) 034619.
[30] A. Daei-Ataollah, O.N. Ghodsi, M. Mahdavi, Phys. Rev. C 97 (2018) 054621.
[31] F. Ghorbani, S.A. Alavi, V. Dehghani, Nucl. Phys. A 1002 (2020) 121947.
[32] N.S. Rajeswari, M. Balasubramaniam, J. Phys. G, Nucl. Part. Phys. 40 (2013) 035104.
[33] N.S. Rajeswari, C. Nivetha, M. Balasubramaniam, Eur. Phys. J. A 54 (2018) 156.
[34] Niyti, Gudveen Sawhney, Manoj K. Sharma, Raj K. Gupta, Phys. Rev. C 91 (2015) 054606.
[35] K.P. Santhosh, I. Sukumaran, Phys. Rev. C 96 (2017) 034619.
[36] K.P. Santhosh, I. Sukumaran, Eur. Phys. J. A 54 (2018) 102.
[37] A.J. Baltz, B.F. Bayman, Phys. Rev. C 26 (1982) 1969.
[38] J.J. Morehead, J. Math. Phys. 36 (1995) 5431.
[39] D.N. Poenaru, W. Greiner, M. Ivascu, D. Mazilu, I.H. Plonski, Z. Phys. A 325 (1986) 435.
[40] K.P. Santhosh, Indu Sukumaran, Phys. Rev. C 96 (2017) 034619.
[41] H. Esbensen, C.N. Davids, Phys. Rev. C 63 (2000) 014315.
[42] Y. Qian, Z. Ren, Eur. Phys. J. A 52 (2016) 68.
[43] V.Y. Denisov, H. Ikezoe, Phys. Rev. C 72 (2005) 064613.
[44] K.-N. Huang, M. Aoyagi, M.H. Chen, B. Crasemann, H. Mark, At. Data Nucl. Data Tables 18 (1976) 243.
[45] F.G. Kondev, M. Wang, W.J. Huang, S. Naimi, G. Audi, Chin. Phys. C 45 (2021) 030001.
[46] W.J. Huang, M. Wang, F.G. Kondev, G. Audi, S. Naimi, Chin. Phys. C 45 (2021) 030002.
[47] M. Wang, W.J. Huang, F.G. Kondev, G. Audi, S. Naimi, Chin. Phys. C 45 (2021) 030003.
[48] I. Sreeja, M. Balasubramaniam, Eur. Phys. J. A 54 (2018) 106.
[49] Jiu-Long Chen, Jun-Yao Xu, Jun-Gang Deng, Xiao-Hua Li, Biao He, Peng-Cheng Chu, Eur. Phys. J. A 55 (2019) 214.
[50] R.K. Gupta, M. Balasubramaniam, C. Mazzocchi, M. La Commara, W. Scheid, Phys. Rev. C 65 (2002) 024601.
[51] R.K. Gupta, R. Kumar, N.K. Dhiman, M. Balasubramaniam, W. Scheid, C. Beck, Phys. Rev. C 68 (2003) 014610.
[52] M. Balasubramaniam, R. Kumar, R.K. Gupta, C. Beck, W. Scheid, J. Phys. G, Nucl. Part. Phys. 29 (2003) 2703.
[53] K.P. Santhosh, P.V. Subha, B. Priyanka, Eur. Phys. J. A 52 (2016) 125.
[54] B. Singh, M.K. Sharma, R.K. Gupta, W. Greiner, Int. J. Mod. Phys. E 15 (2006) 699.
[55] C. Guet, E. Strumberger, M. Brack, Phys. Lett. B 205 (1988) 427.
[56] G. Sauer, H. Chandra, U. Mosel, Nucl. Phys. A 264 (1976) 221.
[57] S.S. Hosseini, H. Hassanabadi, D.T. Akrawy, S. Zarrinkamar, Eur. Phys. J. Plus 133 (2018) 7.
[58] B. Blank, M. Borge, Prog. Part. Nucl. Phys. 60 (2008) 403.
[59] H.R. Jaqaman, Phys. Rev. C 40 (1989) 1677.
[60] G. Royer, J. Mignen, J. Phys. G, Nucl. Part. Phys. 18 (1992) 1781.
[61] K.P. Santhosh, R.K. Biju, Ann. Phys. 334 (2013) 280.
[62] K.P. Santhosh, Phys. Rev. C 104 (2021) 064613.
[63] D.S. Deliona, R.J. Liottab, R. Wyss, Phys. Rep. 424 (2006) 113.

[64] D.S. Delion, R.J. Liotta, R. Wyss, Phys. Rev. Lett. 96 (2006) 072501.
[65] H. Geiger, J. Nuttall, Philos. Mag. 22 (1911) 613.
[66] V. Viola, G. Seaborg, J. Inorg. Nucl. Chem. 28 (1966) 741.
[67] B.A. Brown, Phys. Rev. C 46 (1992) 811.
[68] G. Royer, J. Phys. G, Nucl. Part. Phys. 26 (2000) 1149.